International Scientific Conference 20 UNITECH 26

INTERNATIONAL SCIENTIFIC CONFERENCE
19-21 November 2026
GABROVO

EFFECT OF ANODIZATION PARAMETERS ON PHASE COMPOSITION, SURFACE ROUGHNESS, AND WETTABILITY OF ALUMINUM ALLOY 6063-T6

Deyan Veselinov[1,2], Radostina Yankova[1]

[1] Institute of Metal Science, equipment, and technologies with Center for Hydro- and Aerodynamics "Acad. A. Balevski" at the Bulgarian Academy of Sciences, 67 "Shipchenski prohod" str., Sofia, Bulgaria;

[2]National Center for Mechatronics and Clean Technologies, Sofia, Bulgaria;

**Corresponding author: dveselinov@ims.bas.bg*

Abstract

This study investigates the influence of anodization parameters on the structural, topographical, and wettability characteristics of AA6063-T6 aluminum alloy. A 12-run D-optimal design of experiments was performed to evaluate the effects of current density (3-5 A/dm^{-2}), oxalic acid concentration (0-10 wt.%), electrolyte temperature (10-20 °C), and anodization time (30-60 min) in a 1 M H_2SO_4 electrolyte. The anodized surfaces were characterized by X-ray diffraction (XRD), profilometry and static water contact-angle measurements. XRD patterns were dominated by the characteristic reflections of the aluminum substrate, while no distinct set of intense crystalline oxide peaks was observed, indicating that the anodic layer was predominantly amorphous or weakly nanocrystalline. Increasing current density tended to increase roughness, whereas longer anodization times tended to reduce it. Contact angles ranged from 68.73° to 97.38°, showing that anodization modified the surface from moderately hydrophilic to mildly hydrophobic. Electrolyte temperature and oxalic acid concentration exhibited the strongest positive tendencies toward increased contact angle, although the individual main effects were not statistically significant at $p < 0.05$. Overall, the results demonstrate that anodization modifies AA6063-T6 primarily through changes in surface morphology and wettability, while producing only limited changes in long-range crystalline structure.

Keywords: anodic oxide, anodization parameters, surface characterization, crystallinity, wettability.

INTRODUCTION

Aluminum alloys are widely used in industrial, architectural, and aerospace applications due to their exceptional strength-to-weight ratio, corrosion resistance, and machinability [1]. The 6xxx series of aluminum alloys stands out for its well-rounded performance, offering a combination of moderate strength, outstanding corrosion resistance, and excellent weldability [2]. These alloys are primarily aluminum-magnesium-silicon systems, where the addition of magnesium and silicon results in the formation of the Mg_2Si phase, which is responsible for their strength and hardenability. This makes the 6xxx series highly versatile for applications ranging from structural components to transportation systems [3].

Aluminum alloy 6063-T6, a variant of the 6xxx series, is particularly valued in architectural frameworks, railings, and piping due to its superior extrudability, surface finish, and corrosion resistance [4]. The T6 temper designation enhances its strength and hardness through solution heat treatment and artificial aging, enabling structural applications that require both durability and aesthetic appeal [5]. Compared to other alloys, 6063-T6 balances

This is an open access article licensed under Creative Commons Attribution 4.0 International
Print ISSN: 1313-230X, Online ISSN: 3033-1404

mechanical performance and manufacturability, making it a popular choice in environments requiring long-term performance and design flexibility [6].

To further enhance its surface properties, particularly corrosion resistance and wear durability, anodization is commonly employed. This electrochemical process creates a protective oxide layer on the surface, which can be tailored to meet specific application requirements [7].

Anodization in sulfuric acid electrolytes is widely adopted for its efficiency and ability to produce dense, uniform oxide layers [8]. Modifications to the electrolyte composition, such as the addition of oxalic acid, and process parameters such as current density, temperature, and time, significantly influence the characteristics of the resulting oxide layer. These factors impact key structural and chemical properties, including the oxide's crystallinity, chemical composition, and surface energy. Understanding these relationships is crucial for optimizing anodization conditions to achieve desirable surface characteristics.

This study investigates how anodization parameters affect the phase composition, the topography, and wettability of the oxide layer on aluminum alloy 6063-T6.

EXPOSITION

Experiment and characterization

The material examined in this study was the The material investigated in this study was AA6063-T6 aluminum alloy. Its nominal chemical composition consisted of Mg 0.45–0.90 wt.%, Si 0.20–0.60 wt.%, Fe ≤ 0.35 wt.%, and trace amounts of Cr, Cu, Mn, Ti, and Zn, each ≤ 0.10 wt.%. Other individual elements were limited to ≤ 0.05 wt.% and ≤ 0.15 wt.% in total, with aluminum constituting the balance. Prior to anodization, the specimens were cleaned to remove surface contaminants. The surfaces were sequentially degreased with acetone and isopropyl alcohol, rinsed with deionized water, and dried under ambient conditions.

Anodization was performed in a two-electrode electrochemical cell, with the AA6063-T6 specimen serving as the anode and a pure aluminum sheet as the cathode. The base electrolyte consisted of 1 M sulfuric acid (H_2SO_4), with 10 wt.% oxalic acid added under selected experimental conditions. Four processing parameters were investigated: current density, oxalic acid concentration, electrolyte temperature, and anodization time. The experimental matrix was generated using a design-of-experiments approach in JMP and is presented in Table 1. Current density was varied between 3 and 5 A/dm², oxalic acid concentration between 0 and 10 wt.%, electrolyte temperature between 10 and 20 °C, and anodization time between 30 and 60 min. Continuous electrolyte agitation and cooling were applied during anodization to promote uniform mass and heat transfer and to maintain the prescribed electrolyte temperature.

Table 1. *Experimental design and anodizing conditions*

Sample	Current density (A/dm²)	Oxalic acid *%wt.*	Temperature *°C*	Time *mins*
S01	3	0	10	30
S02	5	0	20	60
S03	5	0	10	30
S04	5	10	10	60
S05	5	10	20	60
S06	3	10	10	30
S07	5	10	20	30
S08	3	0	20	60
S09	5	0	20	30
S10	3	0	10	60
S11	5	10	10	60
S12	3	10	20	30

Phase and structural characterization of the untreated and anodized specimens was performed using a Tongda TDM-10 X-ray diffractometer equipped with Cu Kα radiation. Diffraction patterns were collected in continuous-scan mode over a 2θ range of 20–90° at a scan rate of $1.5° \cdot min^{-1}$. The resulting patterns were analyzed using X'Pert HighScore software (Malvern Panalytical) for peak identification and comparison with reference diffraction data. Because the diffraction response was dominated by the aluminum substrate, minor phase assignments were interpreted

cautiously where potential reflections overlapped with the principal Al peaks.

Surface topography was evaluated using a DGT-SRT200A profilometer (Baxit). The arithmetic mean roughness, Ra, and maximum profile height, Rz, were determined from five independent linear measurements acquired at different locations on each specimen. Multiple measurement positions were used to account for local variations in surface morphology, and the resulting values were used to assess the influence of anodization parameters on surface roughness.

Surface wettability was characterized using a Droplet Lab contact-angle measurement system. A 5 µL droplet of deionized water was deposited onto the specimen surface, and the static contact angle was determined after a stabilization period of 60 s. Three measurements were performed at different locations on each specimen, and the mean value was used for subsequent analysis of surface wettability.

Phase composition

The XRD patterns of the untreated and anodized AA6063-T6 specimens were dominated by the characteristic reflections of face-centered cubic aluminum, with the main peaks located at approximately 38.5–38.9°, 44.8–45.4°, 65.0–65.8°, 77.9–78.8°, and 82.2–83.3° 2θ. These reflections correspond to the Al (111), (200), (220), (311), and (222) crystallographic planes, respectively. A possible phase for the anodic layer is γ-Al_2O_3, as a match with several characteristic reflections was observed.

Changes in the relative intensities and shapes of the Al reflections were evident between the different anodizing conditions; however, these variations did not indicate a systematic crystalline phase transformation. The results therefore suggest that the anodic layer formed under the investigated conditions was predominantly amorphous or weakly nanocrystalline, while the diffraction response remained strongly influenced by the underlying aluminum substrate. Variations in peak intensity should consequently be interpreted cautiously, as they may also reflect crystallographic texture, specimen orientation, or differences in surface geometry.

Overall, the XRD results indicate that changes in current density, oxalic acid concentration, electrolyte temperature, and anodization time primarily affected the structure and morphology of the anodic layer rather than producing clearly distinguishable crystalline oxide phases. This is consistent with the surface roughness and contact-angle measurements, which demonstrate substantial changes in surface characteristics despite the absence of major changes in the crystalline diffraction pattern.

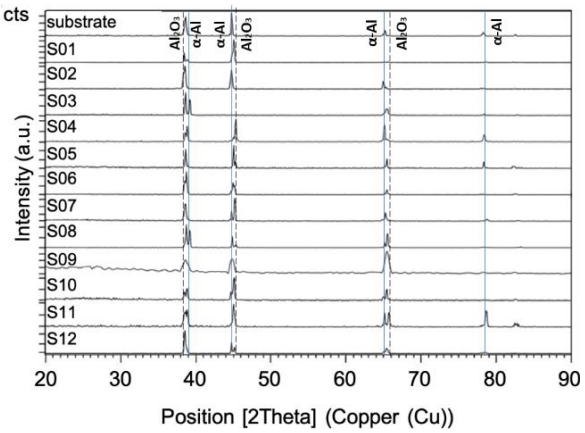


Fig. 1. *XRD patterns of the untreated and anodized AA6063-T6 specimens.*

Surface roughness

The anodized surface morphology, quantified through the parameters of average roughness (Ra) and maximum peak-to-valley height (Rz), showed a clear and systematic dependence on the applied anodization regime (Fig. 2).

The surface roughness of the anodized AA6063-T6 specimens was evaluated using the arithmetic mean roughness (Ra) and maximum profile height (Rz).

The measured values ranged from 0.101 to 0.206 µm for Ra and from 0.788 to 1.515 µm for Rz, indicating that the anodizing conditions produced measurable changes in surface topography. The similar behavior of Ra and Rz suggests that both parameters consistently reflected the evolution of surface morphology.

The DOE response showed that increasing current density tended to increase surface roughness, while the addition of oxalic acid and an increase in electrolyte

temperature produced smaller positive tendencies. In contrast, increasing the anodization time from 30 to 60 min resulted in a reduction in both Ra and Rz, representing the strongest negative effect among the investigated factors. This behavior may reflect the competing processes of oxide growth and electrolyte-assisted dissolution, which can progressively modify and homogenize the surface profile during prolonged anodization.

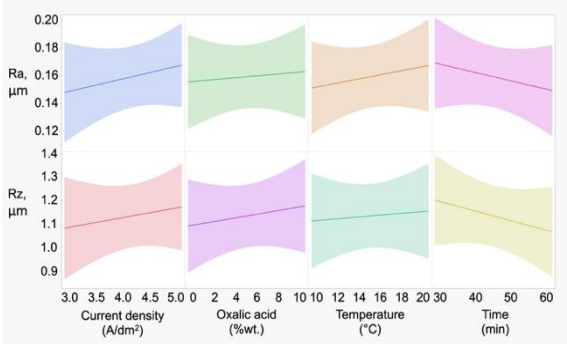


Fig. 2. *Parameters of average roughness (Ra) and maximum peak-to-valley height (Rz) for the anodized surface of Aluminum alloy 6063-T6, depending on the applied anodizing regime.*

Contact angle

The wettability of the anodized AA6063-T6 surfaces was evaluated by static water contact-angle measurements, with the results presented in Fig. 3. The static water contact angle of the anodized surfaces ranged from 68.73° to 97.38°, indicating that the anodization conditions substantially affected surface wettability. Most specimens remained hydrophilic to moderately wetting, while some conditions produced contact angles above 90°, corresponding to mildly hydrophobic behavior. The highest contact angle, 97.38°, was obtained at 5 A/dm², 10 wt.% oxalic acid, 20 °C, and 30 min, whereas the lowest value, 68.73°, occurred at 5 A/dm², 0 wt.% oxalic acid, 10 °C, and 30 min. The DOE response indicated that electrolyte temperature had the strongest positive tendency on contact angle, followed by oxalic acid concentration and anodization time, while current density had only a limited effect.

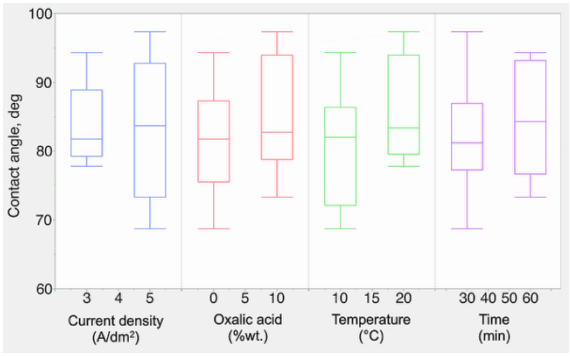


Fig. 3. *Box plots showing the influence of anodizing parameters on the contact angle of anodized aluminium alloy 6063-T6. Each plot displays the median, interquartile range, and outliers for the respective parameter levels, illustrating both central tendencies and variability in wettability response.*

These trends suggest that wettability is influenced primarily by changes in the anodic film chemistry and morphology rather than by current density alone. Moreover, the contact-angle values did not show a clear relationship with the measured Ra and Rz values, indicating that micrometre-scale roughness by itself does not control the wetting behavior. Instead, surface chemistry, pore morphology, and finer-scale topographical features are likely to contribute simultaneously.

CONCLUSION

This work establishes direct processing-structure-property relationships for anodized aluminium alloy 6063-T6 by linking electrolyte composition, current density, temperature, and time to oxide phase evolution, surface roughness, and wettability.

X-ray phase analysis revealed that during anodization in 1 M H_2SO_4 (with or without the addition of 10 wt.% oxalic acid), the aluminum matrix remains the dominant crystalline phase in the analyzed volume.

Quantitative profilometry demonstrated a clear, parameter-dependent evolution of surface topography. Across all conditions, Ra spanned ~0.10-0.21 µm and Rz ~0.84-1.52 µm. The smoothest surface (S01; 3 A/dm², 0 wt.% oxalic acid, 10 °C, 30 min) exhibited Ra = 0.101 µm and Rz = 0.837 µm, indicative of a compact, uniform oxide. In

contrast, pronounced roughening occurred when either oxalic acid (10 wt.%) or higher temperature (20 °C) was applied, with the roughest profile observed for S12 (3 A/dm², 10 wt.% oxalic acid, 20 °C, 30 min; Rz = 1.515 µm, Ra ≈ 0.206 µm). A similarly high Ra (0.206 µm) in S09 (5 A/dm², 0 wt.% oxalic acid, 20 °C, 30 min) underscores that elevated temperature can induce surface coarsening even in the absence of oxalic acid, and that current density accentuates this effect under specific regimes.

Wettability trends mirror these topographical and phase changes. Contact angle measurements increased with the addition of oxalic acid and with higher electrolyte temperature, reflecting a transition toward rougher, more porous surfaces and greater air entrapment at the solid-liquid interface. The highest contact angle (97.383°) was achieved at 10 wt.% oxalic acid and 20 °C for 30 min, whereas the lowest (68.725°) occurred without oxalic acid at 10 °C for 30 min. While current density (3 vs 5 A/dm²) and time (30 vs 60 min) modulated both roughness and contact angle, their effects were comparatively modest and strongly contingent on electrolyte composition and temperature. Taken together, the results indicate that wettability is governed by a synergy between oxide phase development and microstructure: oxalic-acid-assisted and thermally promoted pathways generate rough, porous oxides (higher Ra/Rz) that shift the wetting response toward hydrophobicity, whereas cooler, oxalic-free conditions favor smoother, denser films with lower contact angles.

These findings provide guidelines for surface engineering of AA6063-T6. For applications prioritizing hydrophobicity or self-cleaning behavior, combining oxalic acid with moderate elevation of temperature is an efficient route to high contact angles via controlled roughness and tailored phase assemblages. Conversely, when barrier performance and optical uniformity are paramount, low-temperature, oxalic-free regimes at lower current density yield smoother, more compact oxides. More broadly, the study delivers a coherent framework in which anodizing parameters can be tuned to co-optimize phase composition, roughness metrics, and wetting behavior for targeted functional applications.

ACKNOWLEDGMENTS: *The work in this publication was performed using equipment funded by project BG16RFPR002-1.014-0006 "National Center of Excellence Mechatronics and Clean Technologies".*

REFERENCE

[1] Zheng, J. , Pang, Q. , Hu, Z. , and Sun, Q. Recent Progress on Regulating Strategies for the Strengthening and Toughening of High-Strength Aluminum Alloys. *Materials (Basel, Switzerland)* **2022**, 15

[2] Bhat, K. U. , Panemangalore, D. B. , Kuruveri, S. B. , John, M. , and Menezes, P. L. Surface Modification of 6xxx Series Aluminum Alloys. *Coatings* **2022**, 12, 180.

[3] Yang, Z. , Zheng, X. , Liang, Z. , and Banhart, J. Refreshing Industrially Processed 6xxx Series Aluminum Alloys after Prolonged Natural Aging. *Advanced Engineering Materials* **2023**, 25

[4] Cui, S. , Yu, Y. , Ma, R. , Tian, F. , and Pang, S. Study on Morphology, Microstructure and Properties of 6063-T6 Aluminum Alloy Joints in MIG Welding. *Materials (Basel, Switzerland)* **2023**, 16

[5] Lin, S. , Yuan, M. , Zhao, B. , and Li, B. Out-of-Plane Compression Behaviour of Aluminum Alloy Large-Scale Super-Stub Honeycomb Cellular Structures. *Materials (Basel, Switzerland)* **2023**, 16

[6] Zhang, S. , Liu, X. , Cui, S. , Li, H. , Mo, G. , Li, H. , and Cai, H. Study on the Microstructure and Corrosion Behavior of Dissimilar Aluminum Alloy Welded Joints Formed Using Laser Welding. *Materials (Basel, Switzerland)* **2024**, 17

[7] Scampone, G. and Timelli, G. Anodizing Al-Si Foundry Alloys: A Critical Review. *Advanced Engineering Materials* **2022**, 24

[8] Student, M. M. , Pohrelyuk, I. M. , Hvozdetskyi, V. M. , Veselivska, H. H. , Zadorozhna, Kh. R. , Mardarevych, R. S. , and Dzioba, Yu. V. Influence of the Composition of Electrolyte for Hard Anodizing of Aluminum on the Characteristics of Oxide Layer. *Materials Science* **2021**, 57, 240-247.